Comparison of IEEE802.16e and IEEE802.11n in QPSK with LDPC Minimum Sum Algorithm

Yihua Chen, Huating Syu and Zongyi Saio
Oriental Institute of Technology, Institute of Information and Communication Engineering, New Taipei City, Taiwan

***Abstract*—In accordance with the approximate lower triangular parity check matrix standard of low-density parity-check codes in IEEE Standard 802.16e, this study used LabVIEW to write a variety of adjustable encoding patterns generated at the transmitter end within a single-program structure, including six groups of parity check matrices that were created using the four coding rates in 802.16e, and 114 codewords that were formed by developing 19 types of subblock sizes. A decoder with a minimum sum algorithm was employed to examine the structures of nodes and variable nodes based on changes in the selected standards and complete decoding. This paper describes an encoder–decoder mechanism for combining low-density parity-check codes and minimum sum algorithms, and a quadrature phase-shift keying-channel that was developed and applied to the encoder–decoder mechanism to analyze the resulting bit error rate (BER) curves. The BER curve analyses in 802.16e and 802.11n have revealed that the effect of subblock size on the BER was insignificant, and the two standards exhibited the most similar BERs at the code rates of 5/6 and 2/3; however, the error correction achieved by 802.11n at the code rate of 1/2 was the most effective.**

Keywords-approximate lower triangulation (ALT); low-density parity-check code (LDPC); subblock size; minimum sum algorithm (MSA)

I. INTRODUCTION

In 1948, Claudee Shannon proposed Shannon theory [1], which posits that channel-coding original information bits within the data rate R_b and the channel capacity C effectively reduces the bit error rate (BER) of data transmitted through a channel. The longer a codeword is, the closer the BER data are to infinitesimal; this limit is called the Shannon Limit [2]. Currently, numerous error correction codes [3] have been researched, and the low-density parity-check (LDPC) codes proposed by Gallager [4] have been the most extensively studied. Although the encoding–decoding algorithm of LDPC codes is complex, LDPC codes are a type of error correction code with a data transmission rate that is the closest to the Shannon Limit channel capacity. In the present study, approximate lower triangular (ALT) parity check matrices were combined with the system structure depicted in Fig. 1 to encode information bits and then modulate them by using quadrature phase-shift keying (QPSK) or 16-quadrature amplitude modulation (QAM). The bits were transmitted through additive white Gaussian noise (AWGN) to a receiver, in which the bits were demodulated correspondingly. Finally, the original bits were decoded using a minimum sum algorithm (MSA) [5].

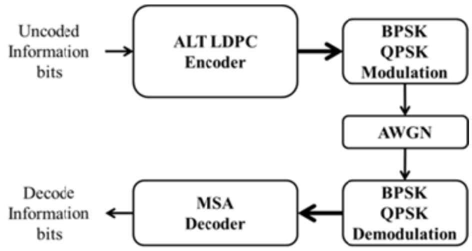

FIGURE I. SCHEMATIC DIAGRAM OF THE ENCODING AND DECODING SYSTEM

The MSA adopted in this study was based on the simplified sum-product algorithm (SPA) [6]. The MSA differs from the SPA in that complex algorithms are not required, thereby accelerating the decoding process.

This study adopted the MSA decoding algorithm used in the ALT encoding standard in the irregular LDPC codes in the 802.16e wireless standards [7]. From the 802.16e standards, four types of code rate were derived to create six groups of parity-check matrices, which were expanded using 19 subblock sizes to form 114 codewords. In this study, the approach used to generate these 114 codewords and the corresponding decoding algorithms were all employed in the program, and the BER curves of a number of specified algorithms were selected for investigation.

II. APPROXIMATE LOWER TRIANGULAR LDPC ENCODER

A. ALT LDPC Parity Check Matrix Structures

LDPC codes are a type of linear block code. Encoding linear block codes typically involves calculating information bit vectors and generating matrices to acquire redundancy bits, which are then added with the information bits to obtain codewords. Decoding involves using the parity check matrices and codeword algorithms to correct errors.

Unlike typical linear block codes, LDPC codes require parity check matrices alone to complete the encoding and decoding process. This study was conducted to improve the encoding approach used in the 802.11n wireless ALT LDPC standard [8], and the same approach was used to accomplish the 802.16e standard encoder. The remainder of this section presents the information regarding the two standards of the parity check matrices.

TABLE I. THE MATRIX SIZES OF THE TWELVE 802.11N ALT LDPC STANDARD PARITY CHECK MATRICES.

Z \ Code rate	1/2	2/3	3/4	5/6
27	324×648	216×648	162×648	108×648
54	648×1296	432×1296	324×1296	216×1296
81	972×1944	648×1944	486×1944	324×1944

TABLE II. THE MATRIX SOZES OF THE SIX 802.16E ALT LDPC STANDARD PARITY CHECK MATRICES

Code Rate	1/2	2/3A	2/3B	3/4A	3/4B	5/6
Matrix Size	12 × 24	8 × 24	8 × 24	6 × 24	6 × 24	4 × 24
24	288 × 576	192 × 576	192 × 576	144 × 576	144 × 576	96 × 576
28	336 × 672	224 × 672	224 × 672	168 × 672	168 × 672	112 × 672
32	384 × 768	256 × 768	256 × 768	192 × 768	192 × 768	128 × 768
36	432 × 864	288 × 864	288 × 864	216 × 864	216 × 864	144 × 864
40	480 × 960	320 × 960	320 × 960	240 × 960	240 × 960	160 × 960
44	528 × 1056	352 × 1056	352 × 1056	264 × 1056	264 × 1056	176 × 1056
48	576 × 1152	384 × 1152	384 × 1152	288 × 1152	288 × 1152	192 × 1152
52	624 × 1248	416 × 1248	416 × 1248	312 × 1248	312 × 1248	208 × 1248
56	672 × 1344	448 × 1344	448 × 1344	336 × 1344	336 × 1344	224 × 1344
60	720 × 1440	480 × 1440	480 × 1440	360 × 1440	360 × 1440	240 × 1440
64	768 × 1536	512 × 1536	512 × 1536	384 × 1536	384 × 1536	256 × 1536
68	816 × 1632	544 × 1632	544 × 1632	408 × 1632	408 × 1632	272 × 1632
72	864 × 1728	576 × 1728	576 × 1728	432 × 1728	432 × 1728	288 × 1728
76	912 × 1824	608 × 1824	608 × 1824	456 × 1824	456 × 1824	304 × 1824
80	960 × 1920	640 × 1920	640 × 1920	480 × 1920	480 × 1920	320 × 1920
84	1008 × 2016	672 × 2016	672 × 2016	504 × 2016	504 × 2016	336 × 2016
88	1056 × 2112	704 × 2112	704 × 2112	528 × 2112	528 × 2112	352 × 2112
92	1104 × 2208	736 × 2208	736 × 2208	552 × 2208	552 × 2208	368 × 2208
96	1152 × 2304	768 × 2304	768 × 2304	576 × 2304	576 × 2304	384 × 2304

Table I lists the matrix sizes of the 12 parity-check matrices in 802.11n, which were generated by combining three types of Z and four types of code rate. Specifically, each matrix generated using each set of Z and code rate was unique. Table II lists the matrix sizes of the six primary parity-check matrices in 802.16e. According to the code-rate differentiation, the Z sizes changed only the postexpansion matrix sizes but not the matrix content.

B. Actualization of the IEEE 802.16e ALT LDPC Parity Check Matrices in LabVIEW

Proposed by Richardson and Urbanke in 2001 [9], ALT LDPC codes involve dividing the established parity check matrix *H* into six submatrices (*A, B, C, D, T,* and *E*) by using algorithmic equations to obtain the redundancy check bits p_1 and p_2, and adding the bits with the original information bit vector *m* to solve the codeword $X = [m\ p_1\ p_2]$. The equations of the redundancy check bits p_1 and p_2 are shown as follows:

$$P_1 = ET^{-1}(Am^T) + Cm^T \quad (1)$$

$$P_2 = T^{-1}\left(Am^T + BP_1{}^T\right) \quad (2)$$

A previous study [8] indicated that fulfilling the IEEE 802.11n wireless ALT LDPC standard involves not only the encoding equations, but also executing the processes, as illustrated in Fig. 2. The processes were adopted to rewrite the 802.16e standard, which was then entered into the LabVIEW platform. Figs. 3 and 4 comprehensively depict the program structure and the packaged Sub VI, respectively.

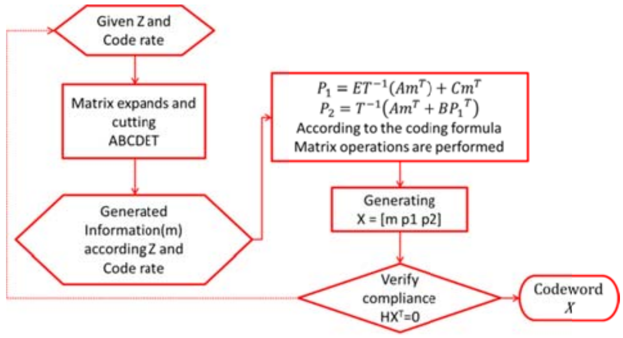

FIGURE II. ALT LDPC ENCODING PROCESS CHART

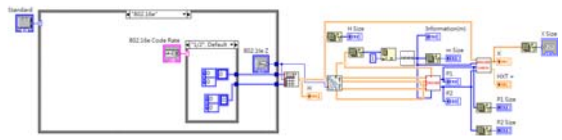

FIGURE III. STRUCTURAL DIAGRAM OF THE ALT LDPC ENCODING PROGRAM

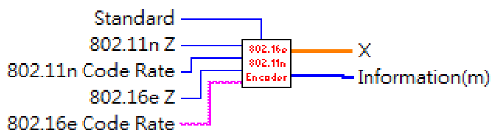

FIGURE IV. COMPREHENSIVE ENCODING PROGRAM SUB VI

In addition to expanding the 802.16e standard, the comprehensive encoding program maintained the 802.11n standard to enable comparing the performance of the decoding algorithms.

III. MINIMUM SUM ALGORITHM

Decoding requires using Tanner graphs [10] and converting the numbers of rows and columns of the parity-check matrices to the variable nodes *B*(*xi*) and check nodes *C*(*xi*). The values 0 and 1 within the matrices were observed, and the variable nodes were connected to the check nodes. Log likelihood ratio (LLR) soft information was transmitted via these connections. However, Table II indicates that within the 802.16e ALT LDPC standard, the sizes of all the check matrices are calculated as percentages. For a detailed description of the decoding approach, the weight (3, 6) regular parity-check matrix in [11] was used as a reference [12]. The matrix was employed to describe the method for generating the Tanner graphs and the processes involved in transmitting the LLR information.

Fig. 5 depicts the four aforementioned steps. Step 1 involved initializing the variable nodes, Step 2 involved updating the LLR soft information at the check nodes, and Step 3 involved updating the LLR soft information at the variable nodes. An evaluation was then conducted to determine whether the designated number of iterations had been fulfilled. If this condition was met, then the hard decision in Step 4 was executed; otherwise, the LLR soft information values at the variable nodes in Step 3 were recalculated at Step 2 in the subsequent iteration until the designated number of iterations was fulfilled. The detail procedure for implementing the MSA circuit by using LabVIEW is demonstrated clearly in Y. H., Chen; et. Al [12].

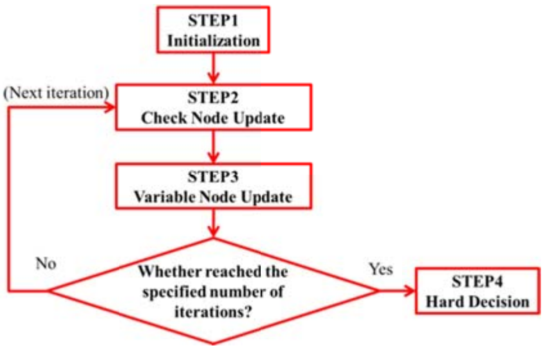

FIGURE V. FLOWCHART OF THE DECODING PROCESS

IV. IEEE 802.11N ALT LDPC STANDARD BER PERFORMANCE ANALYSIS

LabVIEW was employed to simulate the AWGN channel environment with an Eb/No of 0 –1 dB. Each 1 dB interval generated 81 Mb of random data. Table III shows the corresponding relationship between the Eb/No and the σ. The code rates of 1/2, 2/3A, and 5/6 were employed to complete the encoding and decoding process, and QPSK was applied to perform the modulation. Decoding calculation was performed using the MSA iteration.

TABLE III. COMPARISON TABLE OF EB/NO VS. Σ

Eb/No, dB	0	1	2	3	4	5	6	7	8	9	10
σ	0.707	0.630	0.562	0.501	0.446	0.398	0.354	0.316	0.282	0.251	0.224

First, a comparison of the BER curves of Z = 24 bits and Z = 24 bits, both of which exhibited code rates of 5/6, revealed that the curves were nearly entirely overlapped with each other (Fig. 6), indicating that the subblock sizes did not affect the BERs, and that if the code rates were identical, the BERs were nearly identical. However, only the AWGN channel was simulated in this study, and the subblock sizes affected the codeword lengths. Investigating more complex channel environments, such as Rayleigh fading or burst errors, may yield a more comprehensive discourse.

The aforementioned three decoded BER curves obtained from the receiver calculation were compared separately with the BER curve calculated within the 802.11n standard at the same code rate (Figs. 7 and 8), revealing that at the code rates of 5/6 and 2/3, the BER curves of 802.11n and 802.16e were nearly identical (Fig. 7). By the standard of the BER rate of 10^{-5}, the coding gain difference was 0.35 dB at the code rate of 5/6 and < 0.1 dB at the code rate of 2/3.

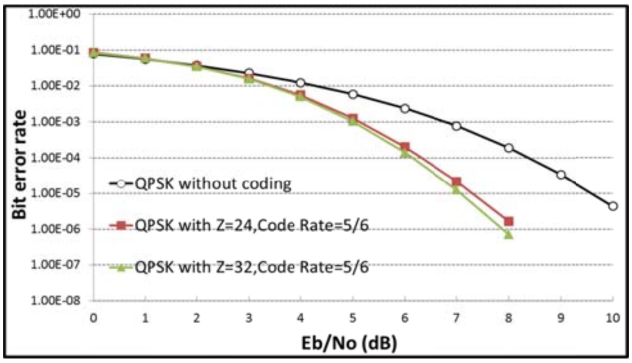

FIGURE VI. COMPARISON OF THE 802.16e BER CURVES AT THE SUBBLOCK SIZE OF 24 AND 32 AND THE CODE RATE OF 5/6.

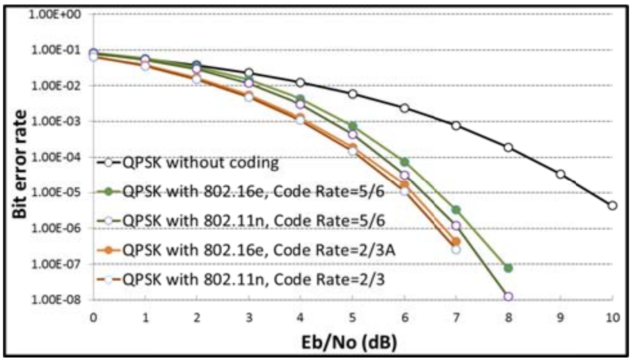

FIGURE VII. COMPARISON OF THE BER CURVES WITH THE 802.16e AND 802.11n CODING AT THE CODE RATES OF 2/3 AND 5/6 TO THE BER CURVE WITHOUT ERROR CORRECTION CODING IN THE LABVIEW SIMULATION INVOLVING THE QPSK MODULATION THROUGH THE AWGN CHANNEL.

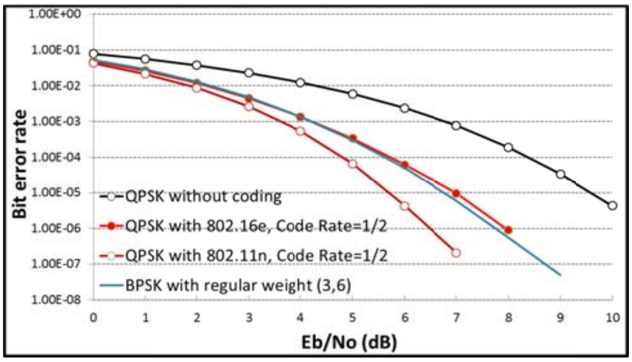

FIGURE VIII. COMPARISON OF THE BER EFFICIENCY WITH THE LDPC CODERS AND DECODERS 802.11n AND 802.16e AT THE CODE RATE OF 1/2 AND THE EFFICIENCY WITH THE REGULAR WEIGHT OF (3,6).

Finally, the BER curves of 802.16e and 802.11n at the code rate of 1/2 were compared to the BER curve with the regular weight of (3,6) from [11] and [13] (Fig. 8). Although both 802.16e and 802.11n were irregular, 802.11n exhibited improved decoding performance. An Eb/No of only 5.7 dB was required for 802.11n to reduce the BER to 10^{-5}, but 802.16e and regular weight (3,6), which exhibited more identical BER curves, required an Eb/No of 7 dB to reduce the BER to 10^{-5}. Thus, the coding gain difference between 802.16e and 802.11n at the code rate of 1/2 was 1.3 dB.

V. CONCLUSION

In this study, a diversified encoder was created using LabVIEW and the IEEE Standard 802.16e irregular parity-check matrices, and the diversified decoder was completed using the MSA. The BER curve diagrams obtained from simulating the AWGN channel with QPSK modulation were compared to the BER curves obtained from previous studies, revealing that the subblock sizes did not affect the BER in the AWGN channel environment. At the code rates of 5/6 and 2/3, the BERs of 80216e and 802.11n were nearly identical. At the BER of 10^{-5}, the coding gain difference was only 0.1 dB; however, at the code rate of 1/2 and the BER of 10^{-5}, the coding gain difference was as high as 1.3 dB. These confirmed that 802.11n exhibited superior error correction ability compared with 802.16e at the code rate of 1/2, and the error correction ability of 802.16e was closer to that of the regular LDPC codes at the code rate of 1/2.

Future studies should consider applying the sum-of-product algorithm or forward–backward algorithm [14], [15] to accomplish decoding. In addition, Rayleigh fading or Ricean fading may be implemented in the channels for further investigation of the changes in BER under various scenarios.

REFERENCES

[1] C. E. Shannon, “A Mathematical Theory of Communication,” Bell Syst. Tech. J, pp. 379-423(Part1);pp. 623-56(Part2), July 1948.

[2] Berrou, C, Glavieux, A,. and Thitimajshima, P., “Near Shannon limit error- correcting coding and decoding: Trubo-codes,” IEEE International Conference on Communications, ICC’93, Geneva. Vol. 2, 1993, pp. 1064-1070. May. 1993.

[3] Brenard Sklar, “Digital Communications Fundamentals and Applications SECOND EDITION”.

[4] R. G. Gallager, “Low-Density Parity-Check Codes, ”IRE Trans. Inform. Theroy, pp. 21-28, Jan. 1962.

[5] Jinghu Chen, Marc P. C., ”Near Optimum Universal Belief Propagation Based Decoding of Low-Density Parity Check Codes”, IEEE Trans Commun., vol. 50, no. 3, pp. 406-414, Mar. 2002.

[6] F. R. Kschischang, B. J. Frey, and H.-A. Loeliger, “Factor graphs and the sum-product algorithm, ”IEEE Trans. Inform. Theory, VOL. 47. pp. 498-519, Feb. 2001.

[7] IEEE P802.11n?/D1.04 Draft Amendment to STANDARD for Information Technology-Telecommunications and information exchange

[8] Yi Hua Chen, Jue Hsuan Hsiao, Zong Yi Siao, “Wi-Fi LDPC Encoder with Approximate Lower Triangular Diverse Implementation and Verification”, Multi-Conference on Systems, Signals & Devices (SSD), 978-1-4799-3866-7/14/$31.00 ©2014 IEEE , pp. 1-6, 2014SSD.

[9] Richardson, T. J, and Urbanke, R. “Efficient encoding of low-density parity-Check Codes, ”IEEE Trans. Inf. Theory, 47. (2), pp. 638-656, 2001.

[10] R. MICHAEL TANNER,”A Recursive Approach to Low Complexity Codes”, IEEE Transactions on information theory, VOL.IT-27, No.5, pp. 533-547 ,September 1981.

[11] Yi-Hua Chen, Chang-Lueng Chu, Jheng-Shyuan He,”FPGA Implementation and Verification of LDPC Minimum Sum Algorithm Decoder with Weight (3, 6) Regular Parity Check Matrix”, ICEMI’2013. pp.682-686. Aug. 2013.

[12] Yi Hua Chen, Jue Hsuan Hsiao, Zong Yi Saio, and Hua Ting Syu , “Minimum Sum Algorithm Decoder for LDPC Nonregular Parity Check Matrix in BPSK System.” PIERS Proceedings, 2136 - 2144, July 6-9, Prague, 2015.

[13] He, Jheng-Shyuan,”Implementation of LDPC Encoder and Decoder on SDR wireless communication system”, Thesis-of-Master-degree, O.I.T Institute of information and communication Engineer, July, 2013.

[14] M. Fossocier, M. Mihaljecvic, H. Imai, “Reduced complexity decoding of low-density parity check codes based on belief propagation, ”IEEE Trans. On Commun., VOL. 47 no. 5, pp. 673-680, May 1999.

[15] L. R. Bahl, J. Cocke, F. Jelinek, and J. Raviv, “Optimal decoding of linear codes for minimizing symbol error rate, ”IEEE Trans. Inform. Theory, VOL. 20, pp. 284-287, Mar. 1974.